ONCOIMMUNOLOGY
2021, VOL. 10, NO. 1, e1873607 (15 pages)
https://doi.org/10.1080/2162402X.2021.1873607

Taylor & Francis
Taylor & Francis Group

ORIGINAL RESEARCH

OPEN ACCESS Check for updates

Addition of anti-TIM3 or anti-TIGIT Antibodies to anti-PD1 Blockade Augments Human T cell Adoptive Cell Transfer

Marina Martinez[a*], Soyeon Kim[a*], Naomi St. Jean[a], Shaun O'Brien[a], Lurong Lian[a], Jing Sun[a], Raluca I. Verona[b], and Edmund Moon[a]

[a]Division of Pulmonary, Allergy, and Critical Care, Perelman School of Medicine at the University of Pennsylvania; [b]Janssen Pharmaceuticals

ABSTRACT

PD1 blockade to reinvigorate T cells has become part of standard of care for patients with NSCLC across disease stages. However, the majority of patients still do not respond. One potential mechanism of resistance is increased expression of other checkpoint inhibitory molecules on T cells leading to their suppression; however, this phenomenon has not been well studied in *tumor-reactive, human* T cells. The purpose of this study was to evaluate this compensatory mechanism in a novel model using human effector T cells infiltrating and reactive against human lung cancer. Immunodeficient mice with flank tumors established from a human lung cancer cell line expressing the NYESO1 antigen were treated with activated human T cells expressing a TCR reactive to NYESO1 (Ly95) with or without anti-PD1 alone and with combinations of anti-PD1 plus anti-TIM3 or anti-TIGIT. A month later, the effect on tumor growth and the phenotype and ex vivo function of the TILs were analyzed. Anti-PD1 and Ly95 T cells led to greater tumor control than Ly95 T cells alone; however, tumors continued to grow. The ex-vivo function of PD1-blocked Ly95 TILs was suppressed and was associated with increased T cell expression of TIM3/TIGIT. Administering combinatorial blockade of PD1+ TIM3 or PD1+ TIGIT with Ly95 T cells led to greater tumor control than blocking PD1 alone. In our model, PD1 blockade was suboptimally therapeutic alone. The effect of TIM3 and TIGIT was upregulated on T cells in response to PD1 blockade and anti-tumor activity could be enhanced when these inhibitory receptors were also blocked with antibodies in combination with anti-PD1 therapy.

ARTICLE HISTORY
Received 9 September 2020
Revised 4 January 2021
Accepted 4 January 2021

KEYWORDS
Checkpoint blockade; TIM3; TIGIT; lung cancer; adoptive T cell therapy

Introduction

Lung cancer remains the leading cause of cancer deaths worldwide despite advances in treatment. Immunotherapy has become a promising treatment strategy. It is well established that tumor-infiltrating lymphocytes (TILs) have the potential to impact the prognosis of lung cancer.[1] However, despite their intra-tumoral presence and reactivity to tumor-associated antigens (TAAs), TILs are functionally impaired, in part due to the expression of the checkpoint inhibitor programmed cell death protein 1 (PD1).[2] PD1 checkpoint blockade in lung cancer has resulted in some remarkable, durable responses in a subset of patients.[3] Currently, PD1 blockade is approved for use in first- and second-line treatment in advanced non-squamous non-small-cell lung cancer (NSCLC).[4]

Unfortunately, many NSCLC patients either do not respond or do so only briefly and then relapse. The mechanisms behind this are being extensively investigated and include many potential factors, including a lack of appropriate T cell infiltration in tumors, infiltration of "bystander" T cells that lack tumor-reactivity, the presence of immunosuppressive cell populations, low mutational burden, epithelial to mesenchymal transition, and tumor mutations like inactivation of the JAK1/2 pathway.[5–8]

One major mechanism is the expression of other inhibitory receptors (IRs) on TILs.[9–13] Lymphocytes that express a tumor-reactive TCR may successfully traffic to and infiltrate into tumors. However, if other IRs are engaged in addition to PD1, PD1 blockade is likely to be insufficient to fully reinvigorate anti-tumor activity. The best studied of these other IRs is CTLA-4 .[14] TIM3 and TIGIT are other IRs that have been shown to mediate CD8 T cell exhaustion, but their exact biochemical functions are not fully known. TIM3 traditionally is thought of as a T cell suppressing receptor[15] but more recently has been shown to stimulate T cells in certain conditions.[16] TIM3 is also involved in macrophage activation[17] and is expressed on Treg cells.[18] TIGIT is another T cell suppressing receptor and it operates in the context of competing receptors, CD226 and CD96. TIGIT is also present on natural killer cells[19,20] and Treg cells.[21] Both IRs can bind to multiple ligands that can be expressed by multiple cell types. Galectin-9, phosphatidylserine (PS), high mobility group box 1 (HMGB1), and cell adhesion molecule 1 (CEACAM1) have been proposed for TIM3; and CD155, CD112, and CD113 for TIGIT.[22–25]

Since checkpoint blockade is aimed at reawakening suppressed T cell populations that bear antigen reactivity via the appropriate TCR repertoire, it is crucial to understand which

CONTACT Edmund Moon Edmund.Moon@uphs.upenn.edu
*these authors contributed equally

Supplemental data for this article can be accessed on the publisher's website.

© 2021 The Author(s). Published with license by Taylor & Francis Group, LLC.
This is an Open Access article distributed under the terms of the Creative Commons Attribution-NonCommercial License (http://creativecommons.org/licenses/by-nc/4.0/), which permits unrestricted non-commercial use, distribution, and reproduction in any medium, provided the original work is properly cited.

checkpoint molecules are active in addition to PD1 on antigen-experienced, tumor-reactive TILs. IR expression and function must be studied in the context of TCR reactivity to TAAs. The blockade of checkpoint molecules on bystander TILs has the drawbacks of 1) requiring higher doses of antibody, as bystander TILs can act as an antibody "sink" and 2) increasing the risk of toxicity by enhancing their reactivity to non-TAAs. Furthermore, checkpoint molecules are varied in their expression dynamics and functional impact and should not be treated equally or interchangeably. Thus, an area that needs to be further investigated is the hierarchy of checkpoint molecules. As an increasing number of checkpoint molecules are discovered on suppressed TILs, we need to better understand which have a dominant effect as combination treatment approaches become increasingly complex with more significant toxicity profiles.

The progress in understanding these issues has been hampered by a lack of robust preclinical models that utilize human cells. Models are necessary because of the difficulty in obtaining tumor biopsies from lung cancer patients who are on checkpoint blockade. Much TIL checkpoint molecule preclinical research has been conducted in mouse models studying *mouse* T cells infiltrating *mouse* cancers.[17,19,26–28] Humanized mice and primates are alternative models but are cost-prohibitive. Furthermore, there are no appropriate primate tumor models. This report utilizes a cost- and time-efficient preclinical model of PD1-blocked *human tumor-reactive* TILs.

Our preclinical model was previously used to demonstrate the ability of PD1-blockade to augment TIL function in lung cancer tumors.[29,30] We used a lung cancer cell line expressing NYESO1 (A549-A2-ESO) to establish subcutaneous flank tumors in immunocompromised (NSG) mice. After tumor engraftment, the mice were intravenously transferred human T cells bearing an optimized TCR (Ly95) reactive against NYESO1.[31] T cells trafficked to and infiltrated into the flank tumors, but became significantly hypofunctional as they upregulated PD1. When mice from this model were treated systemically with pembrolizumab, TILs had enhanced anti-tumor activity, but still did not induce tumor regression.

Given these results, we used this model to ask the following questions: 1) Are other checkpoint molecules besides PD1 causing hypofunction in the tumor-reactive TILs? 2) Does PD1 blockade affect the expression/activity of these other checkpoint molecules? 3) Is one checkpoint molecule dominant in its suppressive effects? And 4) Can we further augment T cell control of flank tumors by combining PD1 blockade with blockade of these other checkpoint molecules?

To answer these questions, we 1) looked for upregulation of IRs on Ly95 T cells after they experienced chronic antigen stimulation in A549-A2-ESO tumors *in vivo*. We also looked for the ability of PD1 blockade to drive compensatory upregulation of other IRs as has been shown in murine TILs by others, and whether PD1 is dominant in its suppressive effects.[32] Consistent with our previous experiments, Ly95 T cells infiltrated the tumors and demonstrated partial anti-tumor activity but did not eliminate the tumors. After harvesting tumors from these mice and isolating the T cells, we identified the tumor-reactive (Ly95+) TILs, then measured the expression of checkpoint molecules and associated T cell function on tumor-reactive versus non-reactive TILs. We demonstrate that TIM3 and TIGIT are upregulated in these TILs and set up two experiments to combine adoptive transfer of tumor-reactive TILs with repeated injections of different combinations of blocking antibodies targeting these detected checkpoint molecules.

This model offers significant advantages in studying checkpoint molecule phenotype patterns and cell-intrinsic mechanisms of T cell hypofunction specific to chronic antigen stimulation, a major limiting factor in solid-tumor-directed immunotherapies. Our data show enhanced anti-tumor efficacy with combination of PD1 blockade with either anti-TIM3 or TIGIT, interesting mechanisms behind these effects, and supports targeting of these checkpoints in the clinic.

Materials and methods

Cell culture conditions

Tumor cell lines and human primary T cells were cultured in RPMI 1640 (Gibco 11875–085) supplemented with 10% heat inactivated fetal calf serum (FCS), 100 U/ml penicillin, 100ug/ml streptomycin sulfate, and 1% L-glutamine (complete cell culture medium).

Generation of the target lung cancer cell line

The human lung cancer cell line A549-CBG was generated by stably transducing the A549 human lung cancer cell line (ATCC CCL185) with a bicistronic third-generation lentiviral vector encoding click beetle green (CBG) luciferase and green fluorescent protein (GFP) (CBG-T2A-GFP).[31] After adding virus to A549 tumor cells in logarithmic growth at an MOI of 5:1, the cells were expanded and flow-sorted for cells that were successfully transduced (GFP-positive). CBG was used in measuring T cell cytolytic activity. The sorted A549-CBG cell line was confirmed to be double-positive for GFP and CBG and then was transduced using a retroviral vector encoding NY-ESO-1-T2A-HLA-A2. The transduced A549-CBG cells were subjected to limiting dilution at 1 cell per well in 96-well plates. Resulting clones were tested by flow cytometry for HLA-A2 expression. HLA-A2 positive clones were selected and co-cultured with Ly95 T cells expressing the NY-ESO-1 TCR. The clones expressing HLA-A2 that induced IFN-γ secretion in Ly95 T cells measured by ELISA were pooled to generate the A549-NY-ESO-1-A2-CBG (referred to in this paper as A549-A2-ESO) cell line. Finally, the A549-A2-ESO cell line was authenticated by ATCC by utilizing Short Tandem Repeat profiling. This was done to confirm that in the process of transducing, enriching, and sorting the A549-A2-ESO cell line, the new cell line was otherwise identical to its parental A549 cell line. (http://www.atcc.org/Services/Testing_Services/Cell_Authentication_Testing_Service.aspx)

Lentivirus preparation

The NY-ESO1-reactive Ly95 TCR construct is an affinity-enhanced variant of the wild-type IG4 TCR identified from T cells recognizing the HLA-A2 restricted NY-ESO-1:157–165

peptide antigen.[31] In the mutant form, the threonine residue at position 95 is substituted by leucine and the serine residue at position 96 is substituted by tyrosine. It was constructed using an overlapping PCR method[33] based on the description and sequences published previously[31] and incorporated into the lentiviral expression vector pELNS bearing the EF1α promoter (provided by Dr. Carl June at the University of Pennsylvania). Packaging of each plasmid into lentivirus has been previously described.[34] Titering of lentiviral concentration was done on Sup-T1 cells (ATCC CRL-1942) at serially decreasing virus dilutions and MOI calculated using a validated formula (June lab, University of Pennsylvania). Transgenic TCR expression was measured by flow cytometry using a PE-conjugated anti-human Vβ13.1 TCR chain antibody (Beckman Coulter, CA).

Isolation, bead activation, lentiviral transduction, and expansion of primary human T-lymphocytes

Primary human $CD4^+$ and $CD8^+$ T cells collected by leukapheresis from healthy volunteer donors at the Hospital of the University of Pennsylvania were obtained from the Human Immunology Core (HIC) at the University of Pennsylvania. All specimens were collected using a University Institutional Review Board-approved protocol. T cells were isolated by negative selection using RosetteSep kits (Stem Cell Technologies, Vancouver, Canada). $CD4^+$ and $CD8^+$ T cells were combined at a 1:1 ratio and cultured in complete cell culture medium in 24-well plates at an initial concentration (at d 0) of 2×10^6 cells per mL, 500 µl per well. They were stimulated at d 0 with magnetic beads coated with anti-CD3 /anti-CD28 (Dynabeads® Human T-Activator CD3/CD28, Thermo Fisher Scientific, MA) at a 1:3 cell to bead ratio. We did not add exogenous IL-2 to the media. After 24 hours, T cells were transduced with the Ly95 TCR using lentiviral vector at an MOI of 5. Cells were counted using a Coulter counter and fed with complete cell culture medium every 48 hours to a concentration of 5×10^5 cells per mL, plated at a density of 3.5×10^5 per cm^2. The beads were removed using a magnet at d 8 after activation. Once T cells became quiescent, as determined by decreased growth kinetics and mean cell size below 350 μm^3, flow cytometry was performed on a small aliquot of 1×10^6 cells to assess transduction efficiency of the Ly95 TCR. The T cells were then either used for functional assays or cryopreserved in optimized T cell freezing media (10% DMSO in FBS, 0.22 µm filtered).

FACS Analysis

Analysis of target tumor cells was conducted by flow cytometry using an APC-conjugated mouse antibody against human HLA-A2 (Biolegend, CA), and a primary mouse monoclonal antibody against NY-ESO-1 (Life Technologies, NY), followed by a PE-conjugated goat anti-mouse secondary antibody (BD Biosciences, CA). T cells were stained for a panel of surface markers using fluorochrome-conjugated antibodies against CD45, CD8, CD4, PD-1 (BD Biosciences, CA), TIM-3 (eBioscience, CA), TIGIT, CD226, CD96, PDL1, galectin-9, Annexin-V, HMGB1, CD155, CD113, and CD112 (Biolegend, CA). Cells were stained for 30 minutes in standard 5 ml round-bottom Falcon FACS tubes (BD Biosciences, CA) in PBS or in BD Horizon brilliant stain buffer (BD Biosciences, CA) and analyzed on a BD™ LSRFortessa (BD Biosciences, CA). All cells were stained for viability using LIVE/DEAD™ Fixable Blue Dead Cell Stain Kit (Thermo Fisher Scientific, MA). Flow cytometry data were analyzed on FlowJo (FlowJo LLC).

Blocking antibodies

The blocking antibodies used were: anti-PD-1 (clone EH12.2H7; mouse-anti-human monoclonal; Ultra-LEAF™, Biolegend, CA; 329958), anti-TIM-3 (goat-anti-human polyclonal; R&D Systems, Minneapolis, MN; AF2365), and anti-TIGIT (clone 741182; mouse-anti-human monoclonal; R&D Systems, Minneapolis, MN; MAB7898). These antibodies have been used for blocking experiments in other published studies and are qualified to be used to block the IRs in these studies.

Flow Cytometric T cell cytokine production assay

Analysis of T cell cytokine production was performed by plating 1×10^6 Ly95 T cells per well on flat-bottom 96-well plates pre-coated with 0.5 µg/ml of anti-CD3 stimulating antibody, in the presence of the protein transport inhibitors monensin (GolgiStop™) and brefeldin A (GolgiPlug™) at the manufacturer recommended concentrations, for 18 hours. PMA (30 ng/ml) and Ionomycin (final concentration 1 µM) were added in a positive control condition. The following day, the cells were harvested and stained for surface markers per the aforementioned surface staining protocol, fixed in 2% paraformaldehyde (PFA), and permeabilized using BD Perm/Wash™ Buffer (BD Biosciences, CA). Intracellular staining for cytokines was done in BD Perm/Wash™ Buffer with fluorochrome-conjugated IFN-γ, IL-2, and TNF-α antibodies (Biolegend, CA).

Luciferase coculture killing assays

For luciferase killing assays, target cells (A549-A2-ESO) were seeded on flat-bottom 96-well plates at a density of 3000 cells per well and left overnight. Isolated T cells were added at determined E:T ratios (20:1, 10:1, and 0:1) and left for 18 hours. After 18 hours, tumor cell lysis was quantified using a Promega Luciferase Assay System and plate-reading luminometer (Promega Corporation, WI).

Measurement of Ly95 T cell IFN-γ secretion by ELISA

Supernatants from 18 hr tumor killing co-culture assays (20:1 and 10:1 effector:target ratios, triplicates for all conditions) were prepared at different dilutions and measured for levels of IFN-γ by standard ELISA protocol (Biolegend, CA).

Animals

All animal experiment protocols were approved and conducted in accordance with the Institutional Animal Care and Use Committee. NOD/scid/IL-2rγ-/- (NSG) mice were bred in

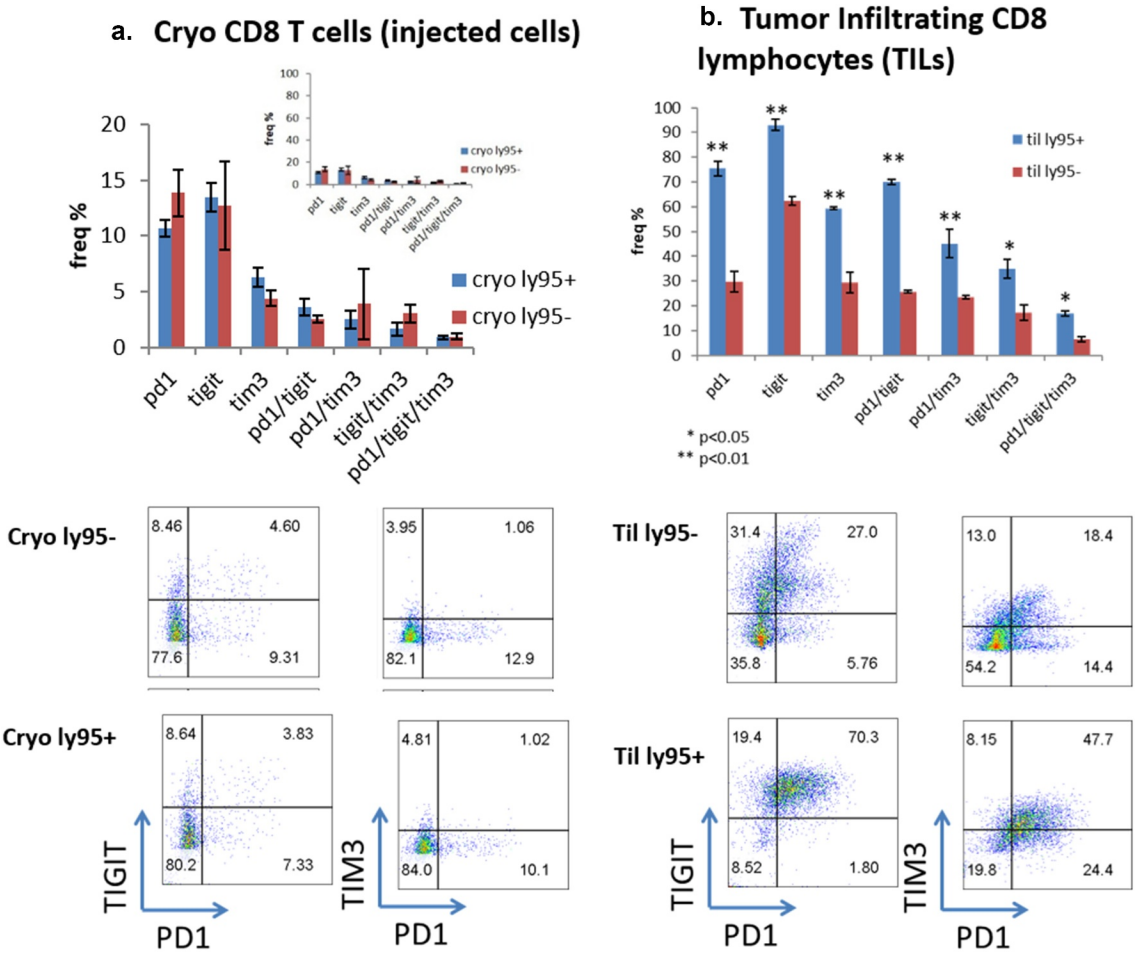

Figure 1. (a) The phenotype of T cells transduced with Ly95 TCR, 10–12 d after activation with anti-CD3/CD28 microbeads is shown: 42.4% expressed the Ly95 TCR; 14%, 5%, and 13% of Ly95- T cells expressed PD1, TIM3, and TIGIT respectively; and 11%, 6%, and 12% of Ly95 + T cells expressed PD1, TIM3, and TIGIT respectively. (Smaller inset graph with Y-axis kept the same as the Y-axis in B) for comparison). (b) Ly95 T cells upregulate PD1, TIM3, and TIGIT after infiltration into A549-A2-ESO flank tumors. 33%, 32%, and 59% of Ly95- T cells expressed PD1, TIM3, and TIGIT respectively. 72%, 56%, and 90% of Ly95 + T cells expressed PD1, TIM3, and TIGIT respectively. Dot plots are representative examples of PD/TIM3/TIGIT expression levels in Ly95 cryopreserved T cells and Ly95 TILs.

the Animal Facility Unit of the Smilow Center for Translational Research at the University of Pennsylvania. Male or female mice were used at 6–8 weeks of age.

In vivo xenograft experiments

A single cell suspension of 5×10^6 A549-A2-ESO tumor cells, in a solution of X–Vivo media (Lonza, NJ) and Matrigel (BD Biosciences, CA), were injected subcutaneously in each of the flanks of NSG mice. Tumor size was measured using calipers and tumor volumes were calculated using the formula $(\pi/6)$ (length) x $(\text{width})^2$. Once tumors were 100–200 mm^3 in size, mice were randomly assigned to one of the following treatment groups for intravenous (IV) tail-vein injection of: (i) saline, (ii) 10×10^6 non-transduced (NTD) T cells, and (iii) 10×10^6 Ly95 expressing T cells. In the experiments combining anti-PD-1, anti-TIM-3, and anti-TIGIT antibody with T cells, additional groups were included in which mice received intraperitoneal (IP) injections of 10 mg/kg of antibody every 5 d. When predefined protocol endpoint of maximum tumor sizes was reached (1,000 mm^3 in any group), tumors were harvested, micro-dissected, and digested in a combination of enzymes according to a previously published protocol optimized for preservation of immune markers.[35] Digested tumors were filtered through 70-µm nylon mesh cell strainers, and red blood cells were lysed with lysing buffer (BD Pharm Lyse; BD Biosciences, CA). Spleens harvested from the same mice were also filtered through 70-µm nylon mesh cell strainers with subsequent red blood cell lysis. After processing, cells from tumor digests and spleens were resuspended in complete media and counted using a hemocytometer. 1×10^6 cells from each single-cell suspension were stained with anti-human CD45, CD8, CD4, and TCRVβ13.1 antibodies to assess the degree of adoptive T cell infiltration. Cells were also stained with anti-human PD1, TIM-3, and TIGIT antibodies to measure expression of IRs on TILs. The *in vivo* experiments were repeated three times in an independent fashion. Groups contained 5–10 mice each.

Ex vivo TIL analysis

After digestion of harvested tumors, necrotic debris was removed from the cell suspension using a Dead Cell Removal Kit (Miltenyi Biotech, CA). TILs were subsequently isolated by positive selection using an anti-human CD45-PE antibody (BD Biosciences, CA) with the EasySEP

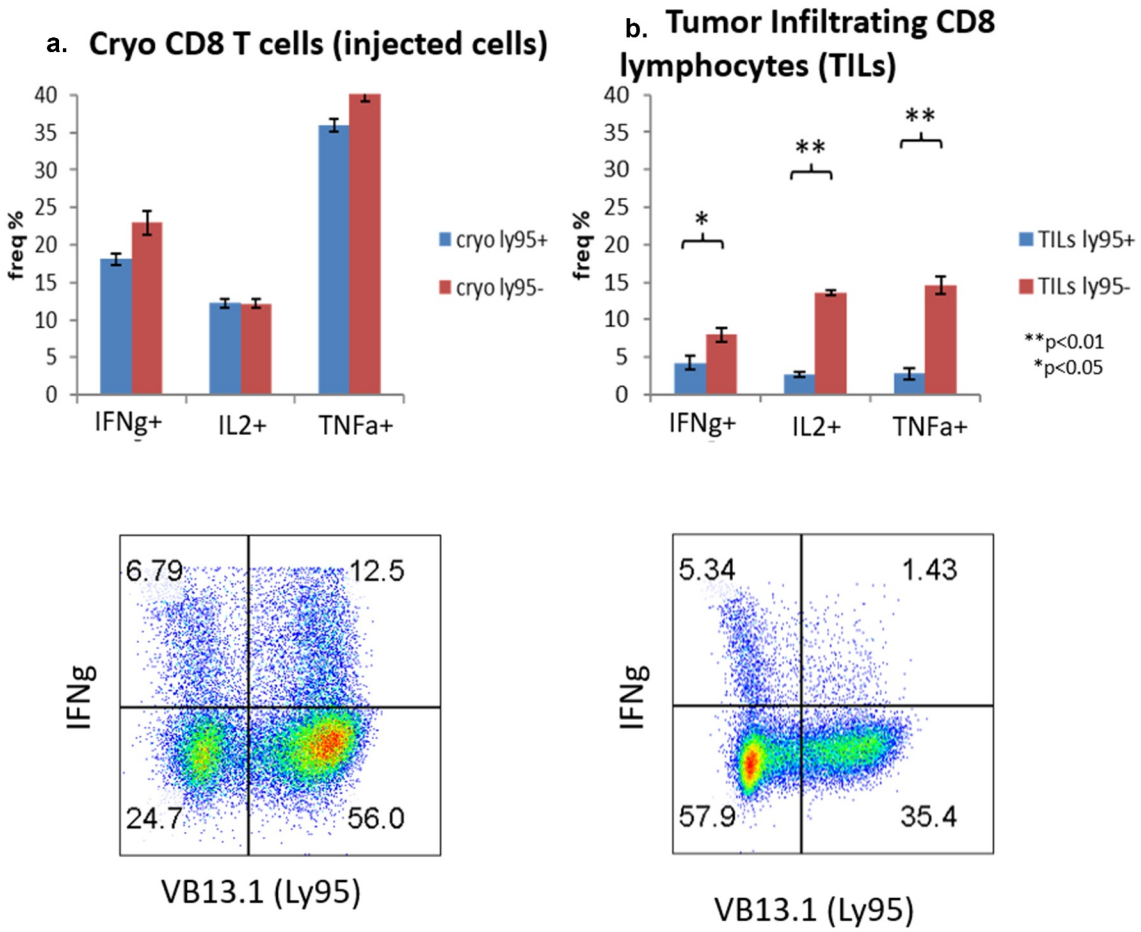

Figure 2. Ly95 TILs (b) isolated from flank tumors are suppressed in their ability to produce IFNg, IL2, and TNFa in response to overnight anti-CD3 stimulation compared to uninjected cryopreserved T cells (a). (Representative dot plots shown.).

PE Selection Kit (STEMCELL Technologies, Vancouver, Canada). Once isolated, functional analyses for TILs were performed in two different ways: (i) luciferase coculture killing assays, and (ii) measurement of antigen-induced T cell IFN-γ secretion by ELISA (see above). Pooling of samples was required in order to isolate sufficient numbers of viable TILs after all processing steps (i.e. harvest, digestion, single cell preparation via filtering and washing, dead cell removal, and CD45 magnetic separation) to perform ex-vivo co-culture killing experiments. When samples were pooled, at least three replicates were maintained within each group for statistics purposes.

Clinical sample processing and analysis:

Malignant pleural effusion (MPE) samples were obtained by thoracentesis from the Harron Lung Center at the Hospital of the University of Pennsylvania following IRB regulations. Samples were processed by centrifugation at 300xg followed by red blood cell lysis (BD Pharm Lyse; BD Biosciences, CA or RBC lysis buffer, SCBiotech, CA). Cells were counted by hemocytometer, and an aliquot of 1×10^6 cells was stained for T cell markers and IRs for flow cytometry. Functional assays for T cell cytokine production (see above) were also done on the cells. Using FlowJo software, cells were gated on live, singlet, CD3+ populations, and IRs were compared on CD8+ and CD4 + cells.

Statistical analysis

All results were expressed as means ± SEM as indicated. For studies comparing two groups, the Student's t-test was used. For comparisons of more than two groups, we used one-way ANOVA with appropriate *post hoc* testing. Differences were considered significant when $p < .05$. Experiments were performed in triplicate and repeated three times in independent fashion.

Disclosure of potential conflicts of interest:

All authors declare no financial or commercial conflict of interest.

Ethics approval

All animal experiments were performed according to guidelines for animal care of the Nijmegen Animal Experiments Committee in accordance with the ethical standards described in the declaration of Helsinki.

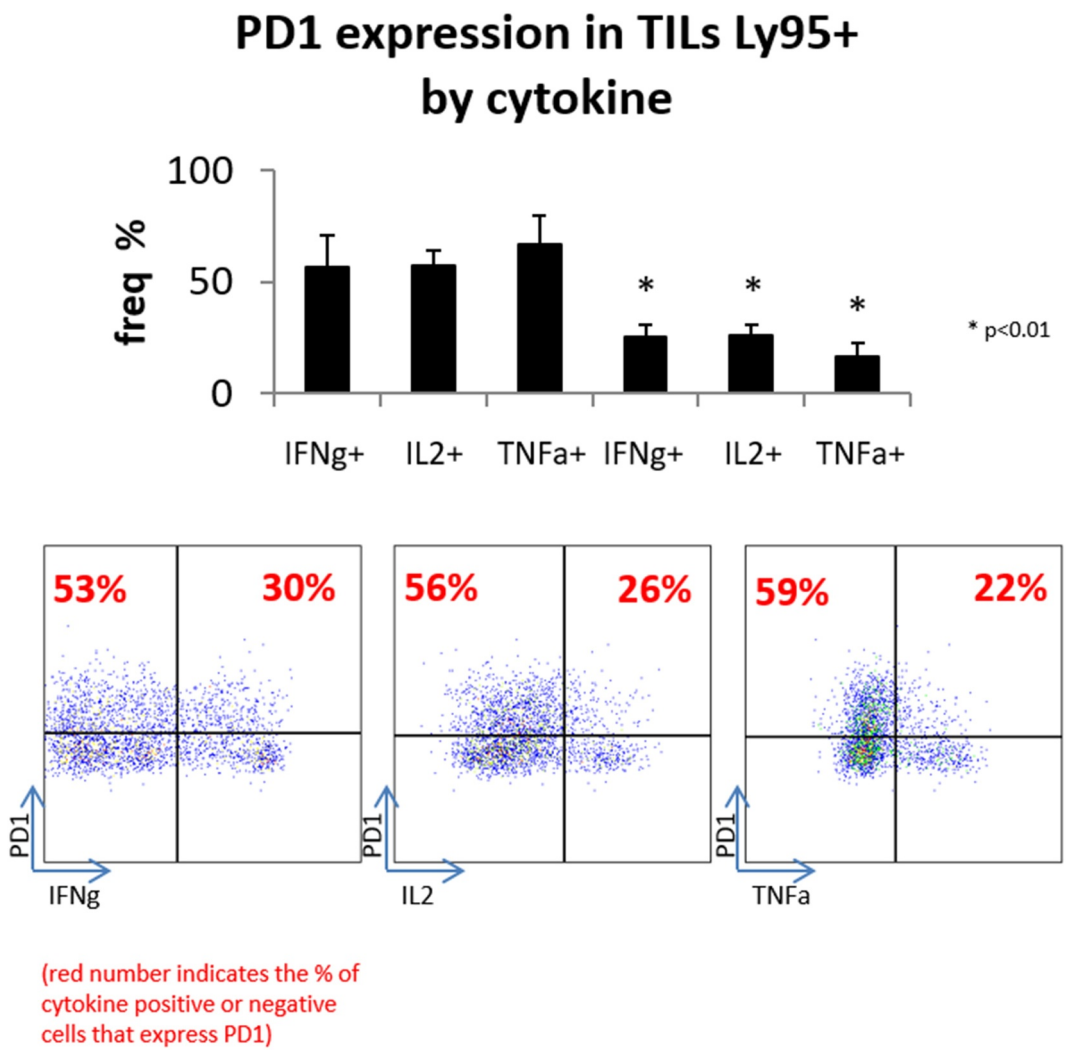

Figure 3. The expression of PD1 correlates with suppression of cytokine production in the TILs isolated from the flank tumors.

Results

Anti-CD3/CD28 bead activated human T cells express low levels of PD1, TIM-3, and TIGIT on both lentiviral transduced and non-transduced populations

We first characterized the IR expression of the injected T cells (called cryopreserved or "cryo" cells) where approximately 50% of the injected T cells expressed the Ly95 transgene and 50% did not ("bystander cells") (**Suppl**. Figure 1a). On the CD8 + T cells, the expression levels of PD1, TIM3, and TIGIT were all quite low (less than 10% of the cells) and there was minimal co-expression of any of these three IRs (PD1, TIM3, and TIGIT). There were no differences between the Ly95+ and Ly95- cells (Figure 1a).

TILs harvested from A549-A2-ESO tumors demonstrate upregulation of three IRs

NSG mice bearing A549-A2-ESO (**Suppl**. Figure 1b) subcutaneous flank tumors ~200 mm^3 in volume were intravenously injected with 10×10^6 Ly95 + T cells. As we have reported[30] (and as shown below), these T cells slowed the growth of tumors by approximately 50%. Approximately 30 d after injection, mice were sacrificed and tumors were harvested, digested, processed into single cell suspension, and evaluated for IR expression by flow cytometry. As seen **in Supplemental** Figure 1c, approximately one-third of the TILs was Ly95 positive with the remainder being bystander cells. There was significant upregulation of all three IRs in the Ly95+ TILs (Figure 1b) compared with the levels observed at the time of injection into the animals (Figure 1a) ($p < .01$). There was also a significant increase in cells expressing multiple IRs. ($p < .05$) Expression of IRs was significantly increased ($p < .05$) on the CD8 T cells that expressed the Ly95 TCR compared to the bystander cells that did not (compare blue columns to red columns).

Ly95+ TILs harvested from A549-A2-ESO tumors demonstrate hypofunction

In addition to phenotype, we also assessed the functional capacity of the injected T cells and those obtained from the tumor by measuring their ability to produce intracellular cytokines after ex vivo crosslinking of their TCRs by plate-bound anti-CD3 antibody. The injected T cells (cryo) and the TILs isolated at approximately 30 d after intravenous adoptive transfer, were cultured for 24 hours in plates coated with a submaximal

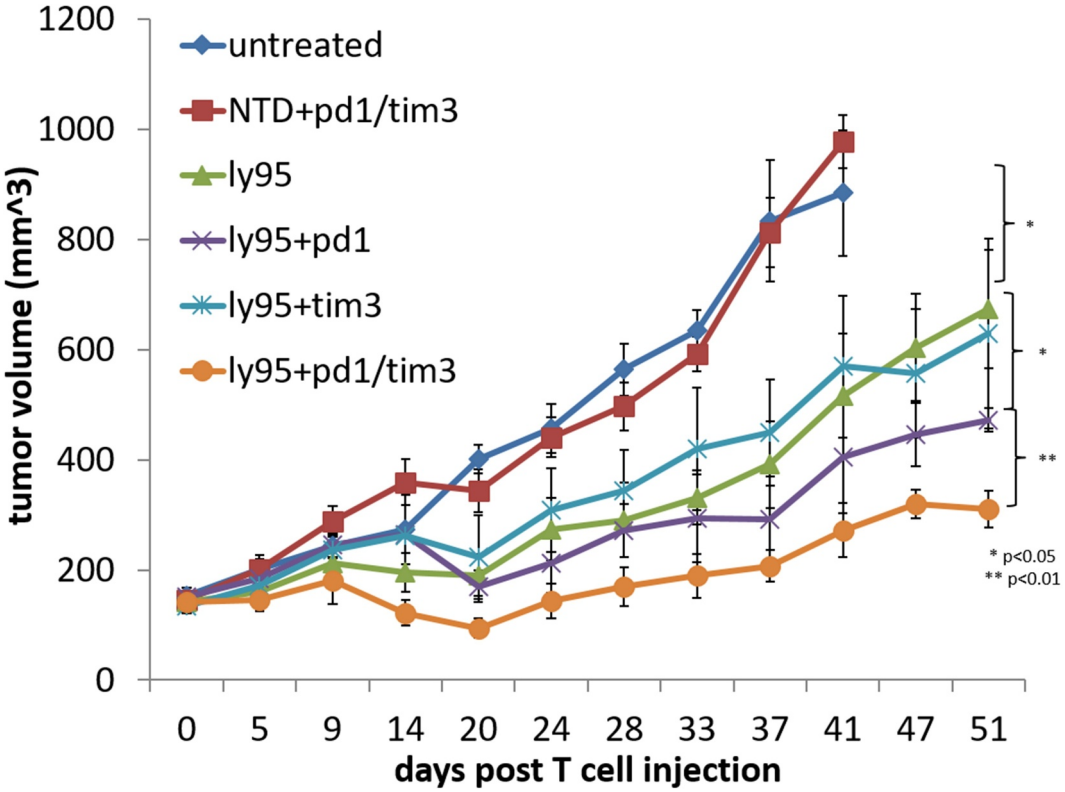

Figure 4. The effect of combinatorial blockade of PD1 and TIM3 on anti-tumor function of adoptively transferred Ly95 T cells on A549-A2-ESO lung cancer flank tumors in-vivo. TIM3 blockade had no effect unless combined with PD1 blockade. (n = 7 in each treatment group) T cells injected IV once on d 0. Antibodies injected IP every 5 d at 10 mg/kg.

(0.5ug/ml) concentration of anti-CD3 antibody in the presence of monensin and brefeldin A. The following day, the cells were stained for the Ly95 TCR and intracellular cytokines.

As seen in Figure 2a, both the Ly95+ and Ly95- infused CD8 cryo T cells were able to produce cytokines in equal amounts. In contrast, the harvested Ly95 TILs were significantly hindered in their ability to make IFN-γ, IL-2, and TNFα in response to anti-CD3 stimulation compared to the cryopreserved control T cells (Figure 2b) ($p < .01$). Furthermore, this hypofunction was significantly greater in the Ly95+ TILs compared to Ly95- TILs (compare blue versus red columns).

To assess the association of PD1 with hypofunction on the Ly95+ TILs, we gated on these cells and then plotted the expression of PD1 versus IFN-γ, IL2, and TNFα. Figure 3 shows that PD1 expression was significantly higher in the CD8 TILs that were not able to produce cytokines versus this those CD8 TILs that did produce intracellular cytokines.

Effect of single and multiple IR blockade in the animal model.

Given our observations that expression of PD1, TIM3 and TIGIT were increased in the Ly95 TILs in our animal model, we hypothesized that single blockade of these IRs or double blockade of these IRs along with anti-PD1 antibody might augment anti-tumor efficacy.

TIM3 and TIM3/PD1 blockade

We first examined the effects of anti-TIM3 antibodies. In this study, A549-NYESO tumor-bearing NSG were untreated or injected with 10 million activated, but non-transduced (NTD) T cells along with injection of anti-PD1 and anti-TIM3 antibodies. We also injected mice with 10 million Ly95 T cells alone or in combination with anti-PD1 antibody, anti-TIM3 antibody, or with both anti-PD1 and anti-TIM3 antibodies and followed tumor size over time (see methods for details). When the experiment's endpoint criteria were met at d 51 post-treatment initiation (Figure 4), we observed: 1) compared to untreated tumors, there was no effect of the NTD T cells/anti-PD1/anti-TIM3 antibodies on tumor growth, 2) as we have previously reported, [30] compared to control, Ly95 T cells significantly reduced the size of the tumors (884 mm^3 vs 674 mm^3; $p < .01$), 3) addition of the anti-TIM3 antibody to Ly95 T cells had no effect (629 mm^3 vs. 674 mm^3, p = NS, 4) as we have previously reported, [30] compared to Ly95 T cells alone, anti-PD1 antibody treatment significantly augmented anti-tumor control (674 mm^3 vs 472 mm^3; $p < .05$), and 5) the combination of PD1 and TIM3 blocking antibodies with Ly95 T cells was significantly better than Ly95 plus only anti-PD1 antibody (310 mm^3 vs. 472 mm^3, $p < .01$).

To explore the mechanisms for this enhanced anti-tumor activity we harvested tumors from each group at the end of the study and conducted further analyses. We first asked how anti-PD1 and anti-TIM3 blockade affected the persistence of TILs within the tumor. As shown in Figure 5a, anti-PD1 treatment significantly ($p < .01$) increased the percentage of CD8 T cells within the tumors. In contrast, anti-TIM3 antibody had no effect on TIL persistence and there was no additional increase to the PD1 effect by the addition of anti-TIM3 antibodies. However, we did note that the expression of TIM3 on the both the Ly95- and Ly95+ TILs was significantly ($p < .01$)

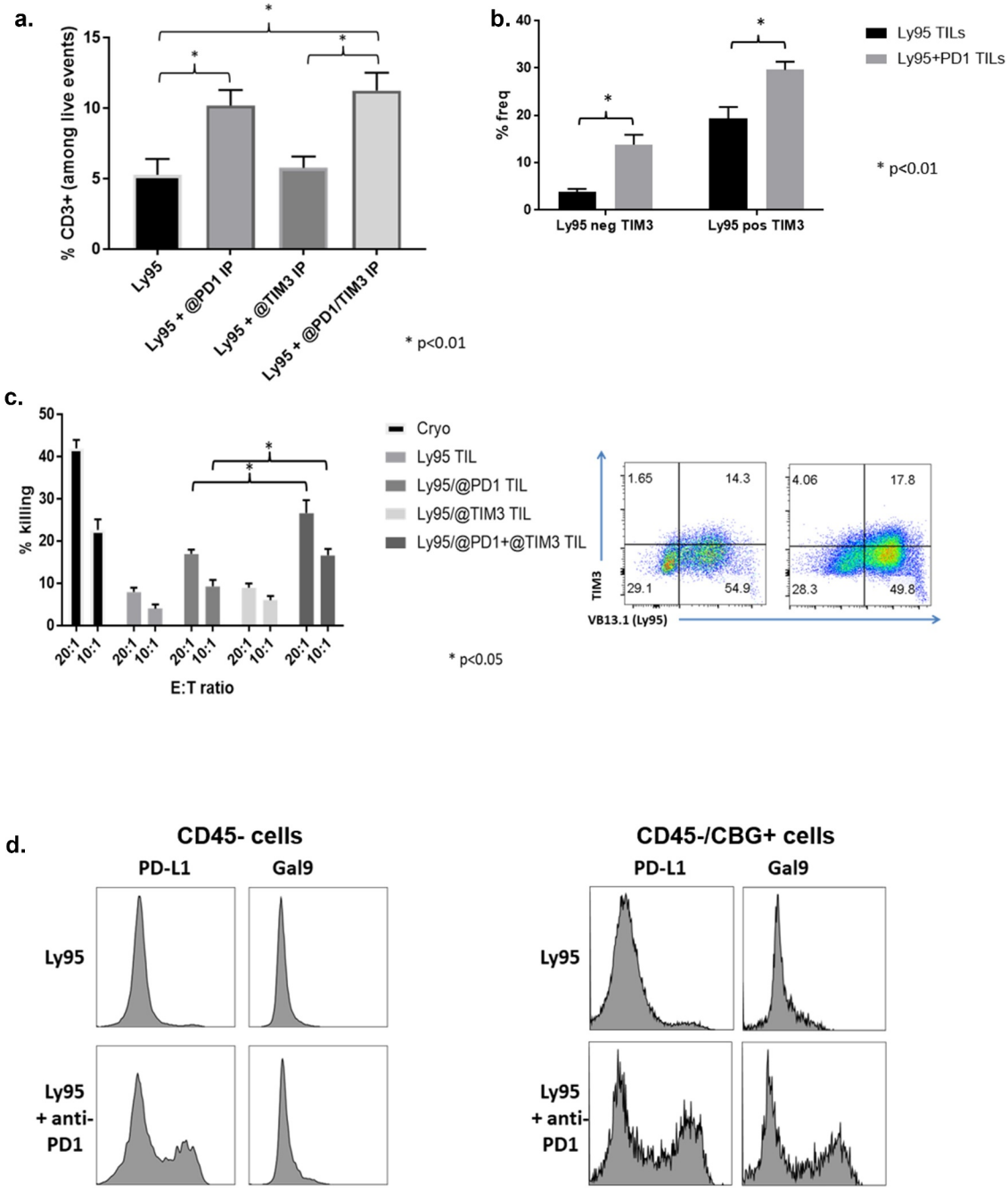

Figure 5. PD1 blockade but not TIM3 blockade increased the frequency of TILs (a). Dual blockade with PD1 and TIM3 did not enhance TIL frequency beyond PD1 single blockade but did enhance the anti-tumor activity as demonstrated by enhanced ex-vivo killing. (b) The expression of TIM3 was upregulated when exposed to PD1 blockade on Ly95+ TILs and Ly95- TILs. Representative dot plots shown. (c) Dual blockade with PD1 and TIM3 enhanced the anti-tumor activity as demonstrated by enhanced ex-vivo killing. (d) Expression of PDL1 and galectin9 on the CD45- cells (tumor and mouse stroma; left set) and CD45-/CBG+ cells (tumor; right set) treated with Ly95 T cells ± PD1 blockade.

increased by anti-PD1 blockade (Figure 5b). We also assessed the function of the TILs by measuring their ability to kill fresh A549-A2-ESO cells ex vivo (Figure 5c). As previously reported, [30] and consistent with the cytokine data above, the isolated TILs killed many fewer tumor cells than the infused cryo T cells at the same E:T ratios. TILs from mice treated with anti-PD1 antibody were significantly more active than TILs alone ($p < .01$) while those treated with only TIM3 antibody were similar to the untreated TILs. However, TILs from mice treated with both anti-PD1 and anti-TIM3 were significantly more active than those from the anti-PD1-treated mice.

We also measured the expression of PD-L1 and Galectin-9 (Gal9), one of the reported ligands of TIM3 on the CD45 negative tumor cells (CBG positive) from the flank tumor digests and observed upregulation of PD-L1, but not Gal9, in the tumors that were treated with Ly95 T cells and PD1 blockade (Figure 5d). Of note, the A549-A2-ESO tumor cell line has very low expression of two other proposed ligands for TIM3, phosphatidylserine and HMGB1 at baseline or after engagement with Ly95 T cells. (Supplemental Figure 2)

These data suggest that TIM3 expression is relatively low on the Ly95 TILs and thus TIM3 blockade has little effect on its

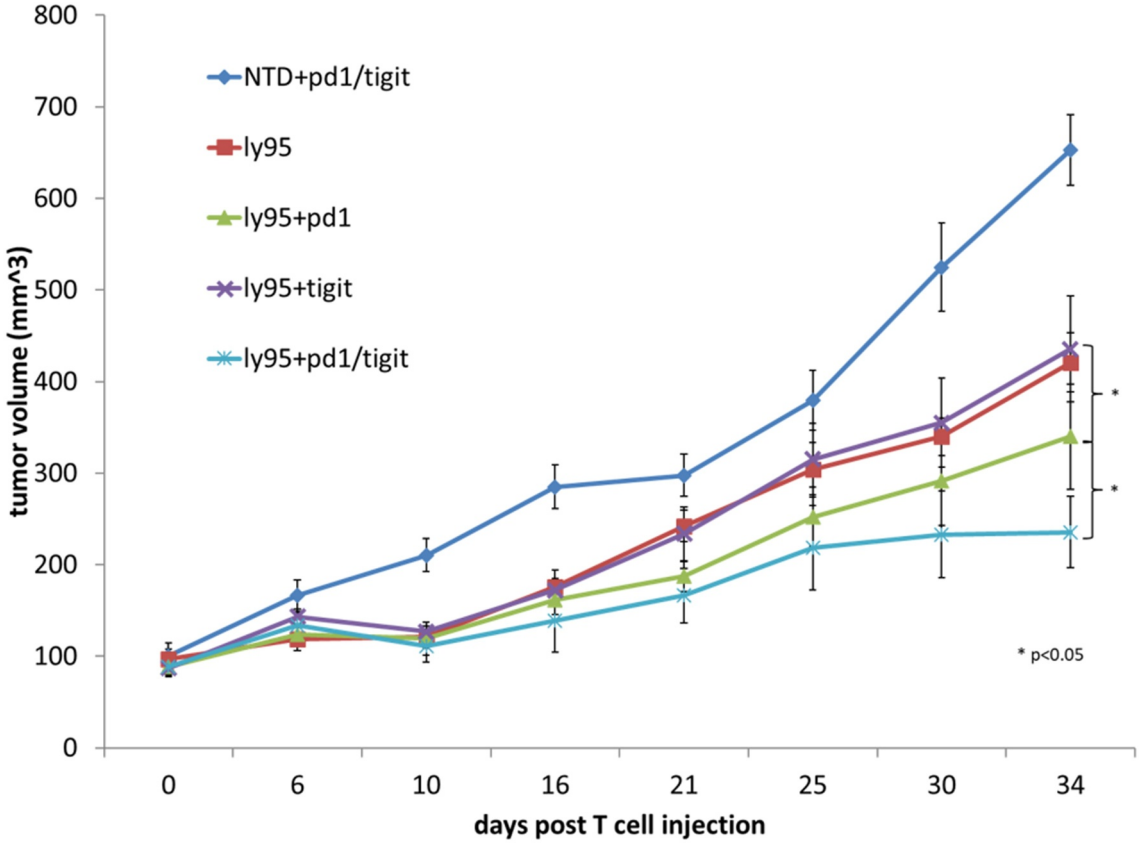

Figure 6. The effect of combinatorial blockade of PD1 and TIGIT on anti-tumor function of adoptively transferred Ly95 T cells on A549-A2-ESO lung cancer flank tumors in-vivo. TIGIT blockade had no effect unless combined with PD1 blockade. (n = 7 in each treatment group) T cells injected IV once on d 0. Antibodies injected IP every 5 d at 10 mg/kg.

own. However, anti-PD1 therapy leads to enhanced TIM3 expression, which induces T cell hypofunction. By blocking TIM3, in the setting of upregulation due to anti-PD1 therapy, augmented anti-tumor effects result.

TIGIT and TIGIT/PD1 blockade

We next examined the effects of anti-TIGIT antibodies. Using the same model, we injected mice with 10 million activated, but non-transduced (NTD) T cells along with injection of anti-PD1 and anti-TIGIT antibodies. We also injected mice with 10 million Ly95 T cells alone, or in combination with anti-PD1 antibodies, anti-TIGIT antibodies, or with both anti-PD1 and anti-TIGIT antibodies and followed tumor size over time (see methods for details). When the experiment's endpoint criteria were met at d 34 post-treatment initiation (Figure 6), we observed: 1) as above, compared to control, Ly95 T cells significantly reduced the size of the tumors (653 mm^3 vs 421 mm^3; $p < .01$), 2) addition of the anti-TIGIT antibody to Ly95 T cells had no effect (436 mm^3 vs. 421 mm^3, p = NS, 4) as above, compared to Ly95 T cells alone, anti-PD1 antibody treatment significantly augmented anti-tumor control (421 mm^3 vs 340 mm^3; $p < .05$), and 5) the combination of PD1 and TIGIT blocking antibodies with Ly95 T cells were significantly better than Ly95 plus only anti-PD1 antibody (236 mm^3 vs. 340 mm^3, $p < .05$).

We harvested tumors from each group at the end of the study and conducted similar analyses as above. As shown in Figure 7a, anti-PD1 treatment ($p < .01$) and anti-TIGIT antibodies significantly ($p < .05$) increased the percentage of CD8 T cells within the tumors. In contrast, to the anti-TIM3 antibody, anti-PD1 had no effect on the expression of TIGIT on the either the Ly95- and Ly95+ TILs, although expression was higher in the Ly95+ cells (Figure 7b). As above, isolated TILs killed significantly ($p < .01$) fewer tumor cells than the infused (cryo) T cells at an E:T ratio of 10:1. TILs from mice treated with anti-PD1 antibody were significantly ($p < .05$) more active, as were those treated with only TIGIT antibody. However, TILs from mice treated with both anti-PD1 and anti-TIGIT were significantly ($p < .01$) more active than those from the anti-PD1 or anti-TIGIT treated mice.

We measured the expression of PD-L1 and the three reported ligands of TIGIT (CD155 (PVR), CD112 (PVRL2, Nectin-2), and CD113 (PVRL3, Nectin-3)) on the CD45 negative tumor cells (CBG positive) from the flank tumor digests and observed upregulation of all four of these ligands in the tumors that were treated with Ly95 T cells and PD1 blockade (Figure 7d). We also measured the expression of the receptors CD226 and CD96 which have been reported to co-express and interact with TIGIT. CD226 counterbalances TIGIT suppression and CD96 competes with CD226 for ligand binding[36] Cryopreserved Ly95 T cells had dual expression of both CD226 and CD96 (47.7%) (Figure 8a first dotplot) with PD1 + Ly95 T cells (Figure 8a second dotplot) having greater dual expression than PD1- counterparts (Figure 8a third dotplot). (80.3% vs. 46.2%). Ly95 TILs had much lower expression of

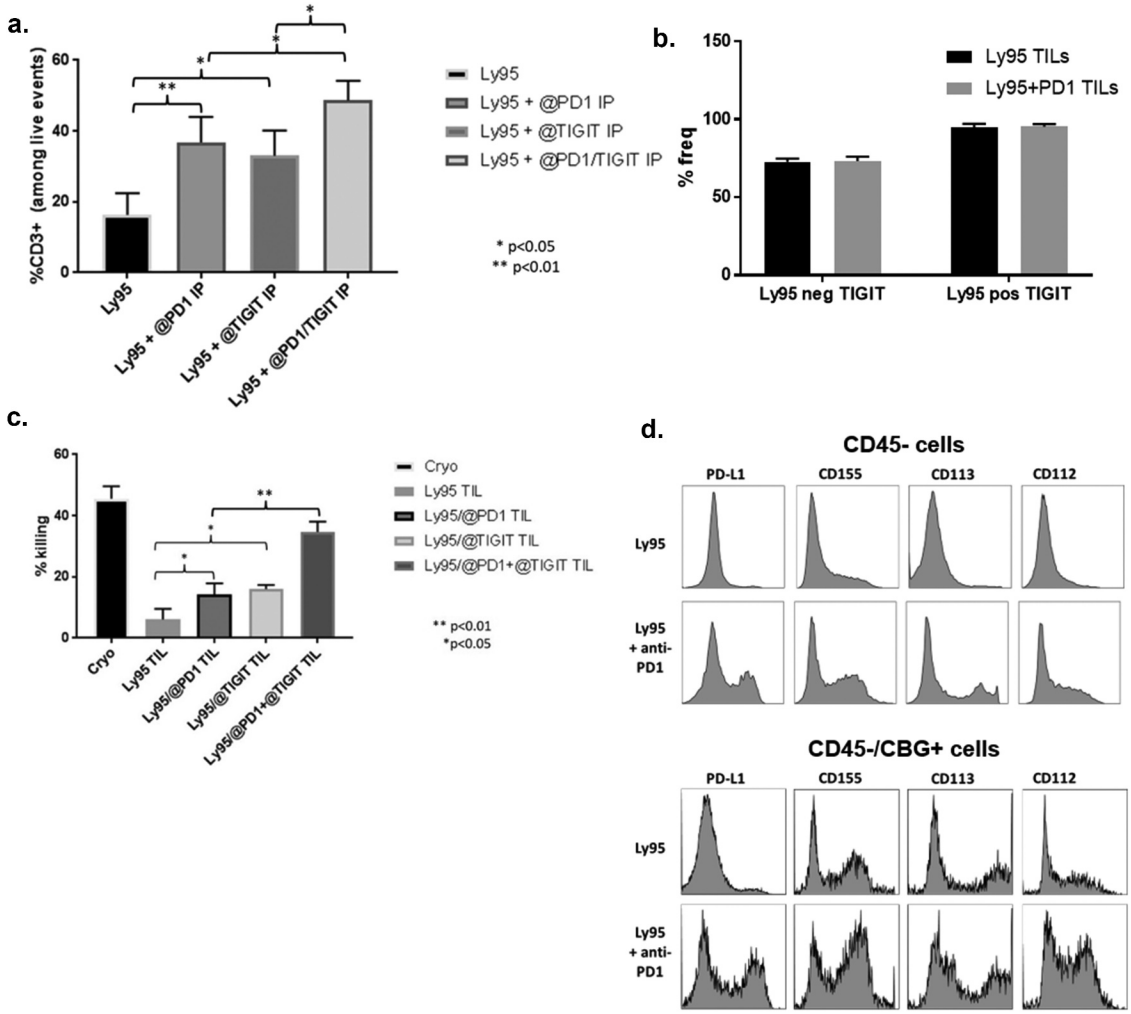

Figure 7. (a) Single blockade by PD1 and TIGIT increased the frequency of TILs. Dual blockade with PD1 and TIGIT enhanced TIL frequency beyond single blockade by either. (b) The expression of TIGIT did not significantly change when exposed to PD1 blockade on Ly95+ TILs and Ly95- TILs. (c) Dual blockade with PD1 and TIGIT enhanced the anti-tumor activity as demonstrated by enhanced ex-vivo killing. (d) Expression of the PDL1, CD155, CD112, and CD112 ligands on the CD45- cells (tumor and mouse stroma; top set) and CD45-/CBG+ cells (tumor; bottom set) treated with Ly95 T cells ± PD1 blockade.

both receptors (5.2%). (Figure 8a, dot plots in blue square; Figure 8b left group of bars), PD1 blockade led to significant upregulation of both CD226 and CD96 (Figure 8a, dot plots in purple square; Figure 8b, red bars).

These data suggest that the mechanisms of anti-TIGIT augmentation of anti-PD1 therapy differ from those of anti-TIM3 augmentation and include: increased numbers of T cells within the tumors, enhancement of T cell function; upregulated TIGIT ligands; and upregulation of co-receptors that share ligands with TIGIT.

TILs isolated from a NSCLC patient's malignant pleural effusion samples before and after pembrolizumab treatment show upregulation of TIM-3, and TIGIT in response to PD1 blockade

Finally, we assessed IR changes on tumor-infiltrating T cells after anti-PD1 therapy in an actual human tumors. Although it is challenging to obtain large enough pre- vs post-anti-PD1 therapy tumor samples that allow detailed TIL analysis, we were able to obtain a pair of malignant pleural effusion samples from a patient with NSCLC before and after treatment with the anti-PD1 antibody, pembrolizumab. After processing, we stained CD3 T cells for expression of IRs (Figure 9). Only 9% of CD8 T cells were expressing TIM3 before therapy; however, this increased markedly to 77% of CD8 T cells after 2 weeks of pembrolizumab treatment (Figure 9a). Before therapy, 50% of the CD8 T cells expressed TIGIT; this increased to 82% of the CD8 T cells after pembrolizumab treatment (Figure 9b) Similar increases were seen in the CD8- T cells (presumably CD4 T cells).

Discussion

Checkpoint blockade has made a dramatic impact in the treatment of cancer patients, with profound and long-lasting responses even in advanced-stage cancers.[37] One of the most targeted checkpoints has been PD1. The first FDA approved anti-PD1 antibody was nivolumab, in 2014, for the treatment of melanoma.[38] Since then, PD1 blockade strategies have expanded to include the use of different antibody clones (pembrolizumab, which targets PD1, and atezolizumab, which targets PD1's main ligand, PDL-1) and to different tumor types,

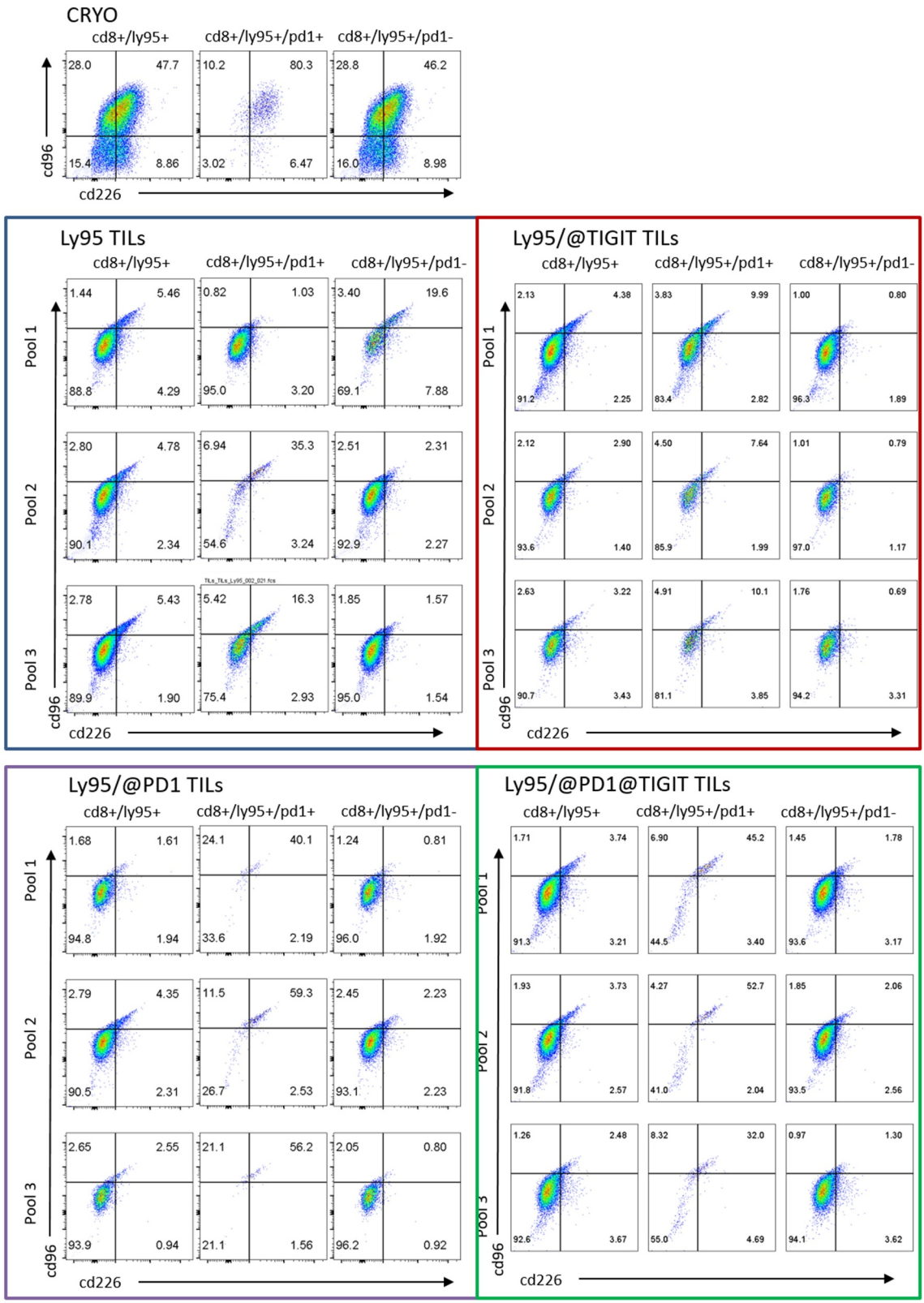

Figure 8. Expression of CD226 and CD96 on Ly95 TILs (top left, in blue), anti-PD1 treated Ly95 TILs (bottom left, in purple), anti-TIGIT treated Ly95 TILs (top right, in red), and anti-PD1+ anti-TIGIT treated Ly95 TILs (bottom right, in green). (a) Frequencies from dotplots summarized in bar graphs. (b).

including non-small cell lung cancer (NSCLC).[39,40] Checkpoint blockade of PD1 has demonstrated added benefit when combined with standard chemotherapy and is approved for use with NSCLC in the first-line setting.[41]

Only about 30% of lung cancer patients who are treated with PD1 checkpoint blockade demonstrate measurable response.[42] The response rate is low despite screening for PDL-1 expression on tumor biopsies to identify patients who are most likely

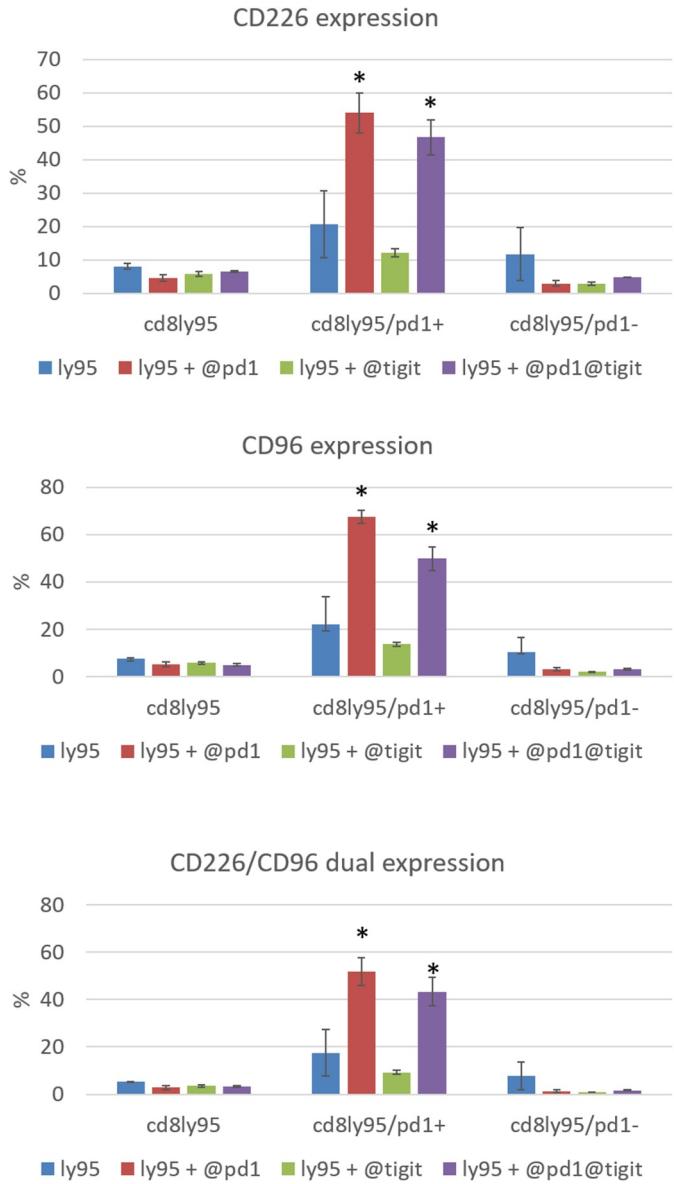

Figure 8b. Expression of CD226 and CD96 on Ly95 TILs (top left, in blue), anti-PD1 treated Ly95 TILs (bottom left, in purple), anti-TIGIT treated Ly95 TILs (top right, in red), and anti-PD1+ anti-TIGIT treated Ly95 TILs (bottom right, in green). (a) Frequencies from dotplots summarized in bar graphs. (b).

to benefit from PD1 checkpoint blockade.[43] Thus, investigators are currently focusing on two significant research initiatives: 1) identifying biomarkers that predict response better than tumor PDL-1 expression and 2) understanding what factors result in escape from anti-PD1 therapy. Our lab is currently investigating these topics in both clinical and lab studies. Specific to escape, we have taken advantage of a unique in vivo model of human TIL hypofunction in which human T cells bearing a TCR (Ly95) reactive to a clinically relevant tumor-associated antigen, NY-ESO-1, traffic and infiltrate into human lung cancer tumors, where they slow tumor progression but undergo profound hypofunction associated with upregulation of PD1. This phenomenon is very similar to what has been described in lung cancer TILs in the clinic.[44–46] When animals are treated with PD1 checkpoint blockade, the anti-tumor function of the Ly95 T cells is improved, but significant hypofunction remains, as evidenced by lack of complete tumor regression.

In the experiments described in this paper, we sought to understand what IR checkpoints in addition to PD1 may contribute to residual hypofunction in TILs. We also wanted to know if PD1 blockade was responsible for compensatory expression of and suppression by other IRs beyond PD1. To answer these questions, we harvested TILs from the flank tumors of mice that were treated with Ly95 T cells and observed two IRs in particular that were significantly upregulated in TILs, in addition to PD1: TIM3 and TIGIT. We next harvested TILs from mice treated with Ly95 T cells with or without PD1 blockade and compared the surface marker phenotype and associated effector function between the two groups. We observed that the expression of TIM3 but not TIGIT was even greater when TILs were treated with PD1 blockade.

We also had the opportunity to see if this in vivo data corresponded with clinical findings. We obtained malignant pleural effusion (MPE) samples before and after pembrolizumab treatment from a patient with NSCLC. By flow cytometry, we observed that T cells in the MPE had significantly greater TIM3 and, to a lesser magnitude, TIGIT expression after PD1 checkpoint blockade treatment. While we only had the ability to obtain these pre- and post-pembrolizumab MPE samples from one patient, this observation is in line with prior published reports of adaptive immune resistance in which there is compensatory upregulation of other IRs when one is blocked. We are actively involved in further research to characterize TILs from MPE samples obtained from NSCLC patients, both receiving and not receiving checkpoint blockade.

After isolating and phenotyping our ex vivo TILs, we performed assays to quantify their function compared to the cells that we injected into the animals (cryopreserved). We observed that the Ly95+ TILs that made the least IFN-γ following overnight anti-CD3 stimulation had dual expression of PD1/TIM3 and PD1/TIGIT. Based on these results, we hypothesized that blocking PD1 in combination with TIM3 or TIGIT would result in greater tumor control than blocking PD1 alone. Thus, we performed two separate animal experiments using dual checkpoint blockade. In the first experiment, we injected tumor-bearing NSG mice with Ly95 T cells in combination with blocking antibodies against PD1, TIM3, or both. In the second experiment, we injected tumor-bearing NSG mice with Ly95 T cells in combination with blocking antibodies against PD1, TIGIT, or both.

In both experiments, blockade of TIM3 or TIGIT alone (without PD1 blockade) had no significant effect on tumor control, but demonstrated effects when blocked with PD1. This made sense for TIM3 since its expression was upregulated in response to PD1 blockade. What was interesting was that TIGIT expression on Ly95+ TILs was very high prior to PD1 blockade and remained at a similar level after PD1 blockade. To understand why TIGIT blockade only had effects when PD1 was blocked we analyzed the level of TIGIT ligands expressed on the tumor cells and indeed saw that the PD1 blockade induced upregulation of these ligands. Additionally, PD1 blockade induced the upregulation of co-receptors that interact with TIGIT, including CD96 which has been shown in murine

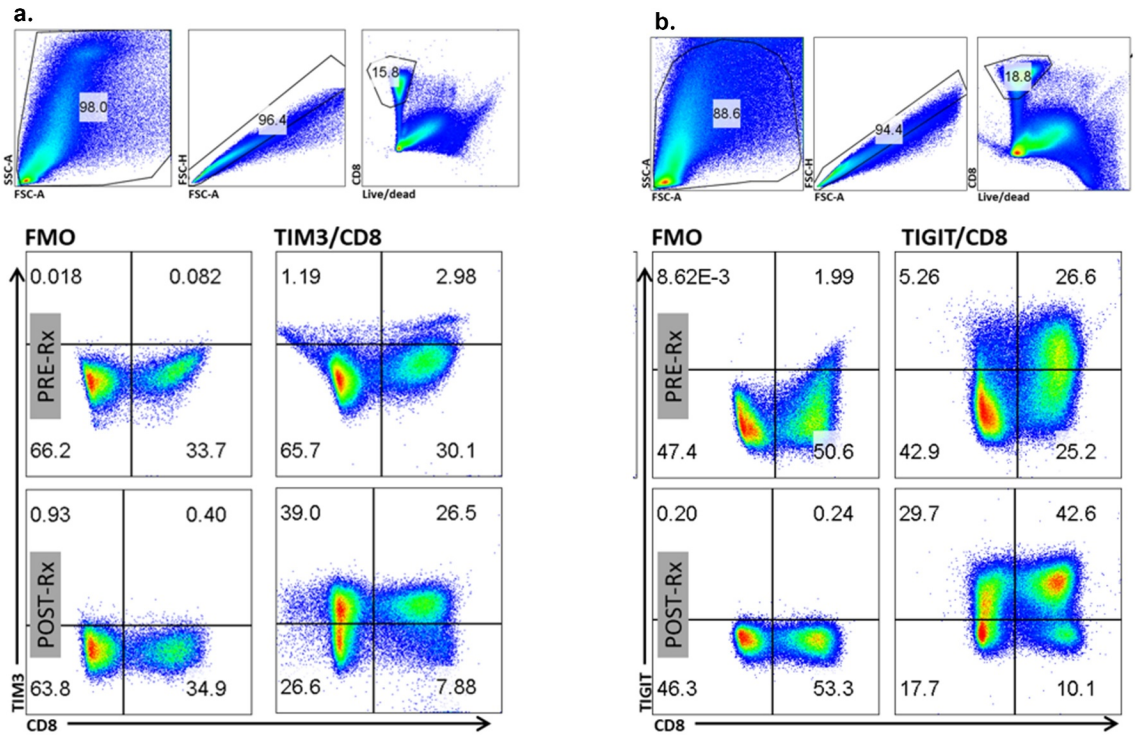

Figure 9. Expression of TIM3 on T cells in NSCLC malignant pleural effusion before and after pembrolizumab treatment. (a) Expression of TIM3 on T cells in NSCLC malignant pleural effusion before and after pembrolizumab treatment. (b) Expression of TIGIT on T cells in NSCLC malignant pleural effusion before and after pembrolizumab treatment.

T cells and murine NK cells.[47,48] Blockade of TIM3 or TIGIT augmented Ly95 anti-tumor function only when combined with PD1 blockade (for both blocking antibodies, tumor sizes were decreased by an average of 1/3 when TIM3 or TIGIT blockade was added to PD1 blockade). These data also support the phenomenon of checkpoint molecule hierarchy with PD1 being a dominant molecule in lung cancer as described by others.[44]

Additional mechanisms of action we focused on were: 1) degree of TIL infiltration, as assessed by flow cytometry and 2) quantification of tumor-lytic function via co-culture killing assays using isolated TILs. Our data suggest that the role of TIM3 blockade in augmenting PD1-blocked Ly95 TIL anti-tumor function is in enhancing tumor-lytic ability after chronic TAA stimulation, rather than enhancing T cell infiltration. In comparison, treatment with TIGIT antibody was observed to enhance both residual tumor-lytic ability and T cell infiltration.

We intentionally focused on the effect of chronic TAA engagement on human TIL IR upregulation and hypofunction. In utilizing an NSG-based xenograft model to do this, the effect of "third-party" immune cell populations, like Tregs, was not studied. We acknowledge that this is one potential weakness of our study. However, our group recently demonstrated that IR suppression is negligibly induced by third-party immune cells. With that being said, we have ongoing parallel studies looking at the interplay of checkpoint blockade and Tregs in a fully mouse system.

The lessons from this study can be summarized in the following four ways: 1) our unique preclinical model has the power to identify targetable combinations of checkpoint molecules in the clinically relevant context of *human tumor-reactive effector T cells* that become *hypofunctional* upon infiltration into *human lung cancer*, 2) both the expression and the function of checkpoint molecules on TILs are important in determining their targetable potential, 3) the expression of checkpoint ligands can be dynamic and are important to analyze, 4) the blockade of either TIM-3 or TIGIT, in combination with PD1 blockade, is an effective way to improve cytokine and cytolytic function and mitigate exhaustion in T cells that do not respond to PD1 blockade alone, and testing these combinations of checkpoint blockade in NSCLC patients warrants investigation.

In conclusion, our study lends significant contribution to the current understanding of immune checkpoint blockade. The field of TIM3 and TIGIT study has relied largely on the use of murine T cells,[17,19,26–28] correlative studies based on analyses of human samples (often in the context of other cancers), [18,49–52] and the context of more immunogenic cancers like melanoma.[20,21,49,50] We describe a unique model of human, tumor-reactive T cells in lung cancer that allows the study of combinatorial checkpoint blockade and its effects on T cell biology and anti-tumor function. Our data support the blockade of TIM3 and TIGIT in combination with PD1 in lung cancer. As clinical trials testing TIM3 and TIGIT blockade are underway, [53,54] our model has the potential to understand the mechanisms behind the response patterns observed and strategies to take advantage of the complex receptor/ligand interactions to promote response.

Funding

This study was funded in part by an R01 from the NCI (R01-CA-219083-03) and a sponsored research agreement with Janssen Pharmaceuticals; National Cancer Institute [R01-CA-219083-03].

References

1. Brambilla E, Le Teuff G, Marguet S, Lantuejoul S, Dunant A, Graziano S, et al. Prognostic Effect of Tumor Lymphocytic Infiltration in Resectable Non-Small-Cell Lung Cancer. J Clin Oncol. 2016;34:1223–1230.
2. Ahmadzadeh M, Johnson LA, Heemskerk B, Wunderlich JR, Dudley ME, White DE, et al. Tumor antigen-specific CD8 T cells infiltrating the tumor express high levels of PD-1 and are functionally impaired. Blood. 2009;114:1537–1544.
3. Gettinger SN, Horn L, Gandhi L, Spigel DR, Antonia SJ, Rizvi NA, et al. Overall Survival and Long-Term Safety of Nivolumab (Anti-Programmed Death 1 Antibody, BMS-936558, ONO-4538) in Patients With Previously Treated Advanced Non-Small-Cell Lung Cancer. J Clin Oncol. 2015;33:2004–2012.
4. Langer CJ, Gadgeel SM, Borghaei H, Papadimitrakopoulou VA, Patnaik A, Powell SF, et al. Carboplatin and pemetrexed with or without pembrolizumab for advanced, non-squamous non-small-cell lung cancer: a randomised, phase 2 cohort of the open-label KEYNOTE-021 study. Lancet Oncol. 2016;17:1497–1508.
5. Shields BD, Mahmoud F, Taylor EM, Byrum SD, Sengupta D, Koss B, *et al*. Indicators of responsiveness to immune checkpoint inhibitors. Sci Rep. 2017;7:807.
6. Rizvi NA, Hellmann MD, Snyder A, Kvistborg P, Makarov V, Havel JJ, et al. Cancer immunology. Mutational landscape determines sensitivity to PD-1 blockade in non-small cell lung cancer. Science. 2015;348:124–128.
7. Shin DS, Zaretsky JM, Escuin-Ordinas H, Garcia-Diaz A, Hu-Lieskovan S, Kalbasi A, et al. Primary Resistance to PD-1 Blockade Mediated by JAK1/2 Mutations. Cancer Discov. 2017;7:188–201.
8. Zaretsky JM, Garcia-Diaz A, Shin DS, Escuin-Ordinas H, Hugo W, Hu-Lieskovan S, et al. Mutations Associated with Acquired Resistance to PD-1 Blockade in Melanoma. N Engl J Med. 2016;375:819–829.
9. Abate-Daga D, Hanada K, Davis JL, Yang JC, Rosenberg SA, Morgan RA. Expression profiling of TCR-engineered T cells demonstrates overexpression of multiple inhibitory receptors in persisting lymphocytes. Blood. 2013;122:1399–1410.
10. Baitsch L, Legat A, Barba L, Fuertes Marraco SA, Rivals JP, Baumgaertner P, et al. Extended co-expression of inhibitory receptors by human CD8 T-cells depending on differentiation, antigen-specificity and anatomical localization. PLoS One. 2012;7:e30852.
11. Blackburn SD, Shin H, Haining WN, Zou T, Workman CJ, Polley A, *et al*. Coregulation of CD8+ T cell exhaustion by multiple inhibitory receptors during chronic viral infection. Nat Immunol. 2009;10:29–37.
12. Drake CG. Combined Immune Checkpoint Blockade. Semin Oncol. 2015;42:656–662.
13. Phan TG, Long GV, Scolyer RA. Checkpoint inhibitors for cancer immunotherapy. Multiple checkpoints on the long road towards cancer immunotherapy. Immunol Cell Biol. 2015;93:323–325.
14. Ribas A, Wolchok JD. Cancer immunotherapy using checkpoint blockade. Science. 2018;359:1350–1355.
15. Banerjee H, Kane LP. Immune regulation by Tim-3. F1000Research. 2018;7:316.
16. Huang YH, Zhu C, Kondo Y, Anderson AC, Gandhi A, Russell A, et al. CEACAM1 regulates TIM-3-mediated tolerance and exhaustion. Nature. 2015;517:386–390.
17. Monney L, Sabatos CA, Gaglia JL, Ryu A, Waldner H, Chernova T, et al. Th1-specific cell surface protein Tim-3 regulates macrophage activation and severity of an autoimmune disease. Nature. 2002;415:536–541.
18. Gao X, Zhu Y, Li G, Huang H, Zhang G, Wang F, et al. TIM-3 expression characterizes regulatory T cells in tumor tissues and is associated with lung cancer progression. PloS One. 2012;7:e30676.
19. Yu X, Harden K, Gonzalez LC, Francesco M, Chiang E, Irving B, et al. The surface protein TIGIT suppresses T cell activation by promoting the generation of mature immunoregulatory dendritic cells. Nat Immunol. 2009;10:48–57.
20. JM C, Ka M, Pagliano O. IL15 Stimulation with TIGIT Blockade Reverses CD155-mediated NK-Cell Dysfunction in Melanoma. Clin Cancer Res. 2020;26:5520–5533.
21. Fourcade J, Sun Z, Chauvin JM, Ka M, Davar D, Pagliano O, et al. CD226 opposes TIGIT to disrupt Tregs in melanoma. JCI Insight. 2018;3.
22. Wolf Y, Anderson AC, Kuchroo VK. TIM3 comes of age as an inhibitory receptor. Nat Rev Immunol. 2020;20:173–185.
23. Harjunpaa H, Guillerey C. TIGIT as an emerging immune checkpoint. Clin Exp Immunol. 2020;200:108–119.
24. Casado JG, Pawelec G, Morgado S, Sanchez-Correa B, Delgado E, Gayoso I, et al. Expression of adhesion molecules and ligands for activating and costimulatory receptors involved in cell-mediated cytotoxicity in a large panel of human melanoma cell lines. Cancer Immunol Immunother. 2009;58:1517–1526.
25. Mendelsohn CL, Wimmer E, Racaniello VR. Cellular receptor for poliovirus: molecular cloning, nucleotide sequence, and expression of a new member of the immunoglobulin superfamily. Cell. 1989;56:855–865.
26. Levin SD, Taft DW, Brandt CS, Bucher C, Howard ED, Chadwick EM, *et al*. Vstm3 is a member of the CD28 family and an important modulator of T-cell function. Eur J Immunol. 2011;41:902–915.
27. Sakuishi K, Apetoh L, Sullivan JM, Blazar BR, Kuchroo VK, Anderson AC. Targeting Tim-3 and PD-1 pathways to reverse T cell exhaustion and restore anti-tumor immunity. J Exp Med. 2010;207:2187–2194.
28. Stanietsky N, Simic H, Arapovic J, Toporik A, Levy O, Novik A, et al. The interaction of TIGIT with PVR and PVRL2 inhibits human NK cell cytotoxicity. Proc Natl Acad Sci U S A. 2009;106:17858–17863.
29. Liu X, Ranganathan R, Jiang S, Fang C, Sun J, Kim S, et al. A Chimeric Switch-Receptor Targeting PD1 Augments the Efficacy of Second-Generation CAR T Cells in Advanced Solid Tumors. Cancer Res. 2016;76:1578–1590.
30. Moon EK, Ranganathan R, Eruslanov E, Kim S, Newick K, O'Brien S, et al. Blockade of Programmed Death 1 Augments the Ability of Human T cells Engineered to Target NY-ESO-1 to Control Tumor Growth after Adoptive Transfer. Clin Cancer Res. 2016;22:436–447.
31. Robbins PF, Li YF, El-Gamil M, Zhao Y, Wargo JA, Zheng Z, et al. Single and dual amino acid substitutions in TCR CDRs can enhance antigen-specific T cell functions. J Immunol. 2008;180:6116–6131.
32. Koyama S, Akbay EA, Li YY, Herter-Sprie GS, Buczkowski KA, Richards WG, et al. Adaptive resistance to therapeutic PD-1 blockade is associated with upregulation of alternative immune checkpoints. Nat Commun. 2016;7:10501.
33. Ho SN, Hunt HD, Horton RM, Pullen JK, Pease LR. Site-directed mutagenesis by overlap extension using the polymerase chain reaction. Gene. 1989;77:51–59.
34. Carpenito C, Milone MC, Hassan R, Simonet JC, Lakhal M, Suhoski MM, et al. Control of large, established tumor xenografts with genetically retargeted human T cells containing CD28 and CD137 domains. Proc Natl Acad Sci U S A. 2009;106:3360–3365.
35. Quatromoni JG, Singhal S, Bhojnagarwala P, Hancock WW, Albelda SM, Eruslanov E. An optimized disaggregation method for human lung tumors that preserves the phenotype and function of the immune cells. J Leukoc Biol. 2015;97:201–209.
36. Chan CJ, Martinet L, Gilfillan S, Souza-Fonseca-Guimaraes F, Chow MT, Town L, et al. The receptors CD96 and CD226 oppose each other in the regulation of natural killer cell functions. Nat Immunol. 2014;15:431–438.

37. Pacheco JM, Camidge DR, Doebele RC, Schenk EA. Changing of the Guard: immune Checkpoint Inhibitors With and Without Chemotherapy as First Line Treatment for Metastatic Non-small Cell Lung Cancer. Front Oncol. 2019;9:195.
38. Topalian SL, Sznol M, McDermott DF, Kluger HM, Carvajal RD, Sharfman WH, et al. Survival, durable tumor remission, and long-term safety in patients with advanced melanoma receiving nivolumab. J Clin Oncol. 2014;32:1020–1030.
39. Herbst RS, Baas P, Kim DW, Felip E, Perez-Gracia JL, Han JY, et al. Pembrolizumab versus docetaxel for previously treated, PD-L1-positive, advanced non-small-cell lung cancer (KEYNOTE-010): a randomised controlled trial. Lancet. 2016;387:1540–1550.
40. Rittmeyer A, Barlesi F, Waterkamp D, Park K, Ciardiello F, von Pawel J, et al. Atezolizumab versus docetaxel in patients with previously treated non-small-cell lung cancer (OAK): a phase 3, open-label, multicentre randomised controlled trial. Lancet. 2017;389:255–265.
41. Addeo A, Banna GL, Metro G, Di Maio M. Chemotherapy in Combination With Immune Checkpoint Inhibitors for the First-Line Treatment of Patients With Advanced Non-small Cell Lung Cancer: A Systematic Review and Literature-Based Meta-Analysis. Front Oncol. 2019;9:264.
42. Santini FC, Hellmann MD. PD-1/PD-L1 Axis in Lung Cancer. Cancer J. 2018;24:15–19.
43. Cottrell TR, Taube JM. PD-L1 and Emerging Biomarkers in Immune Checkpoint Blockade Therapy. Cancer J. 2018;24:41–46.
44. Thommen DS, Schreiner J, Muller P, Herzig P, Roller A, Belousov A, et al. Progression of Lung Cancer Is Associated with Increased Dysfunction of T Cells Defined by Coexpression of Multiple Inhibitory Receptors. Cancer Immunol Res. 2015;3:1344–1355.
45. Prado-Garcia H, Romero-Garcia S, Aguilar-Cazares D, Meneses-Flores M, Lopez-Gonzalez JS. Tumor-induced CD8+ T-cell dysfunction in lung cancer patients. Clin Dev Immunol. 2012;2012:741741.
46. O'Brien SM, Klampatsa A, Thompson JC, Martinez MC, Hwang WT, Rao AS, et al. Function of Human Tumor-Infiltrating Lymphocytes in Early-Stage Non-Small Cell Lung Cancer. Cancer Immunol Res. 2019;7:896–909.
47. Blake SJ, Stannard K, Liu J, Allen S, Yong MC, Mittal D, et al. Suppression of Metastases Using a New Lymphocyte Checkpoint Target for Cancer Immunotherapy. Cancer Discov. 2016;6:446–459.
48. Mittal D, Lepletier A, Madore J, Aguilera AR, Stannard K, Blake SJ, et al. CD96 Is an Immune Checkpoint That Regulates CD8(+) T-cell Antitumor Function. Cancer Immunol Res. 2019;7:559–571.
49. Chauvin JM, Pagliano O, Fourcade J, Sun Z, Wang H, Sander C, et al. TIGIT and PD-1 impair tumor antigen-specific CD8(+) T cells in melanoma patients. J Clin Invest. 2015;125:2046–2058.
50. Fourcade J, Sun Z, Benallaoua M, Guillaume P, Luescher IF, Sander C, et al. Upregulation of Tim-3 and PD-1 expression is associated with tumor antigen-specific CD8+ T cell dysfunction in melanoma patients. J Exp Med. 2010;207:2175–2186.
51. Johnston RJ, Comps-Agrar L, Hackney J, Yu X, Huseni M, Yang Y, et al. The immunoreceptor TIGIT regulates antitumor and antiviral CD8(+) T cell effector function. Cancer Cell. 2014;26:923–937.
52. Guillerey C, Harjunpaa H, Carrie N, Kassem S, Teo T, Miles K, et al. TIGIT immune checkpoint blockade restores CD8(+) T-cell immunity against multiple myeloma. Blood. 2018;132:1689.
53. Tiragolumab Impresses in Multiple Trials. Cancer Discov. 2020; 10: 1086.
54. Davar D, Boasberg P, Eroglu Z, Falchook G, Gainor J, Hamilton E, et al. A Phase 1 Study of TSR-022, an Anti-TIM-3 Monoclonal Antibody, in Combination with TSR-042 (Anti-PD-1) in Patients with Colorectal Cancer and Post-PD-1 NSCLC and Melanoma [abstract]. In: Proceedings of the 33rd Annual Meeting of the Society of Immunotherapy of Cancer; 2018 Nov 7–11; Washington, D.C